International Journal of Heat and Mass Transfer 51 (2008) 5838–5843

Contents lists available at ScienceDirect

International Journal of Heat and Mass Transfer

journal homepage: www.elsevier.com/locate/ijhmt

Boundary layer flow over a shrinking sheet with power-law velocity

Tiegang Fang *

Mechanical and Aerospace Engineering Department, North Carolina State University, 3182 Broughton Hall, Campus Box 7910, 2601 Stinson Drive, Raleigh, NC 27695, United States

ARTICLE INFO

Article history:
Received 22 January 2008
Received in revised form 26 April 2008
Available online 1 July 2008

Keywords:
Similarity solution
Stretching surface
Shrinking sheet
Power-law velocity
Analytical solution
Numerical solution

ABSTRACT

In this work, the boundary layers over a continuously shrinking sheet with a power-law surface velocity and mass transfer were investigated. Based on the boundary layer assumptions, the similarity equations with a controlling parameter β were obtained and solved numerically. Theoretical analysis was conducted for certain special conditions and exact solutions were derived for $\beta = -1$ and $\beta = -2$ and also for the power index $m = -1$. Numerical techniques were used to solve the similarity equation for other parameters. Quite different and interesting solution behaviors were found for a shrinking sheet compared with a stretching sheet. Multiple solutions were obtained for certain mass transfer parameter and controlling parameter β. Velocity overshoot near the wall and near the boundary layer edge were observed for certain solution branches. The current results for a power-law shrinking sheet offer quite interesting nonlinear behaviors and greatly enrich the solution and understanding of boundary layers.

1. Introduction

The flow induced by a stretching boundary is important in the extrusion processes in plastic and metal industries [1–3]. The pioneering work in this area was carried out by Sakiadis [4,5]. Sakiadis analyzed the boundary layer assumptions and the governing equations of the problem, and the boundary layer flow on a continuously stretching surface with a constant speed was investigated. His work was further verified by Tsou et al. [6] experimentally. Following these works, the boundary conditions on the surface were generalized by other researchers [7–18]. The velocity of the surface was changed to be a function of distance from the slot, where the surface was stretched out. A power-law velocity function was the most common case. Thermal boundary conditions included a power-law surface temperature or a power-law surface heat flux. Mass transfer such as fluid suction and injection was also considered on the stretching surface. Exponentially stretching velocity and rapidly decreasing velocity conditions were also discussed [14–16]. The effect of radiative heating on a moving sheet was studied through numerical simulation [17]. A new solution branch for both impermeable and permeable stretching sheets was found by Liao [18,19], which indicates that multiple solutions for the stretching surfaces are possible under certain conditions. Recently, a paper was published by Miklavcic and Wang [20] to investigate the flow over a shrinking sheet. For this flow configuration, the fluid is stretched toward a slot and the flow is quite different from the stretching case. It is also shown that mass suction is required generally to maintain the flow over the shrinking sheet. In their paper, 2D and axis-symmetric conditions were discussed and those solutions are fortunately the exact solutions of the Navier–Stokes equations. The shrinking sheet problem was also extended to other fluids [21,22]. For this new type of shrinking flow, it is essentially a backward flow as discussed by Goldstein [23]. For a backward flow configuration, namely the surface moving from $+\infty$ to the slot, the fluid loses any memory of the perturbation introduced by the leading edge, say the slot. Therefore, the flow induced by a shrinking sheet shows quite distinct physical phenomena from the forward stretching flow. A search on the literature about this flow showed few publications on this subject since it is quite a new type of flow. The objective of this paper is to extend the shrinking sheet problem to a more general situation with a power-law velocity of the sheet shrinking into the slot. The effects of the power index on the wall drag and flow behavior will be discussed.

2. Mathematical formulation

Consider a steady, two-dimensional laminar flow over a continuously shrinking sheet in a quiescent fluid. The sheet shrinking velocity is $U_w = -U_0 x^m$ and the wall mass suction velocity is $v_w = v_w(x)$, which will be determined later. The x-axis runs along the shrinking surface in the direction opposite to the sheet motion and the y-axis is perpendicular to it. Based on the boundary layer assumption the governing equations of this problem become

* Tel.: +1 919-5155230; fax: +1 919-5157968.
E-mail address: tfang2@ncsu.edu

0017-9310/$ - see front matter © 2008 Elsevier Ltd. All rights reserved.
doi:10.1016/j.ijheatmasstransfer.2008.04.067

Nomenclature

a	a constant in the analytical solutions related to the mass transfer parameter
a_1	an integration constant
a_2	an integration constant
f	dimensionless free stream function
f'	the first derivative of f with respect to η
f''	the second derivative of f with respect to η
f'''	the third derivative of f with respect to η
m	power exponent for the wall velocity distribution
s	mass transfer parameter at the sheet
u	fluid velocity in x direction
v	fluid velocity in y direction
v_w	fluid velocity in y direction at the sheet
x	coordinate along the shrinking sheet pointing to the opposite direction of sheet motion
y	coordinate perpendicular to the x direction
C	a constant in the solution equal to $f(\infty)$ for $\beta = 1$
C_0	an integration constant
U_0	constant in the sheet shrinking velocity
U_w	sheet shrinking velocity

Greek symbols

β	control parameter $\beta = \frac{2m}{m+1}$
α	dimensionless wall stress, $f''(0)$
η	similarity variable
ν	kinematic viscosity
φ	newly defined the stream function for large mass suction
$\dot{\varphi}$	the first derivative of φ with respect to ω
$\bar{\varphi}$	the second derivative of φ with respect to ω
$\ddot{\varphi}$	the third derivative of φ with respect to ω
ψ	stream function
ω	defined new variable

$$\frac{\partial u}{\partial x}+\frac{\partial v}{\partial y}=0, \tag{1}$$

$$u\frac{\partial u}{\partial x}+v\frac{\partial v}{\partial y}=\nu\frac{\partial^2 u}{\partial y^2} \tag{2}$$

with the boundary conditions

$$u(x,0)=-U_0x^m, \tag{3a}$$

$$v(x,0)=v_w(x), \tag{3b}$$

$$u(x,\infty)=0. \tag{3c}$$

where u and v are the velocity components in the x and y directions respectively, ν is the kinematic viscosity. The stream function and similarity variable can be posited in the following form:

$$\psi(x,y)=f(\eta)\sqrt{\frac{2}{m+1}\nu x U_0 x^m} \tag{4a}$$

and

$$\eta=y\sqrt{\frac{m+1}{2}\frac{U_0x^m}{\nu x}}. \tag{4b}$$

With these definitions, the velocities are expressed as $u=U_0x^mf'(\eta)$ and

$$v=-\sqrt{\frac{m+1}{2}U_0\nu x^{m-1}}\left[f'(\eta)\eta\frac{m-1}{m+1}+f(\eta)\right].$$

The wall mass transfer velocity becomes

$$v_w(x)=-\sqrt{\frac{m+1}{2}U_0\nu x^{m-1}}f(0)\propto x^{(m-1)/2}.$$

The similarity equation is obtained as follows:

$$f'''+ff''-\beta f'^2=0 \tag{5}$$

with the boundary conditions (BCs)

$$f(0)=s, \tag{6a}$$

$$f'(0)=-1, \tag{6b}$$

$$f'(\infty)=0, \tag{6c}$$

where s is the wall mass transfer parameter showing the strength of the mass transfer at the sheet and $\beta=2m/(m+1)$. But the above derivation does not apply to the case with $m=-1$. When $m=-1$, the similarity solution reads

$$f'''+f'^2=0 \tag{7}$$

with the same BCs as Eq. (6a)–(6c), where the stream function is $\psi(x,y)=f(\eta)\sqrt{\nu U_0}$ and the similarity variable is $\eta=(y/x)\sqrt{U_0/\nu}$. However, the wall suction velocity for this particular is always zero even though s is not zero. For $-1\leqslant m\leqslant\infty$, it is obtained $-\infty\leqslant\beta\leqslant 2$. In addition, for situations with $-\infty\leqslant m\leqslant -1$, namely the rapidly decreasing velocity cases, the stream function and the similarity variable have to be redefined as

$$\psi(x,y)=f(\eta)\sqrt{\frac{-2}{m+1}}\nu U_0x^{(m+1)/2} \tag{8a}$$

and

$$\eta=y\sqrt{\frac{m+1}{-2}\frac{U_0}{\nu}}x^{(m-1)/2}. \tag{8b}$$

With these definitions, the velocities are re-expressed as $u=U_0x^mf'(\eta)$ and

$$v=\sqrt{\frac{m+1}{-2}U_0\nu x^{m-1}}\left[f'(\eta)\eta\frac{m-1}{m+1}+f(\eta)\right].$$

Then the wall mass transfer velocity becomes

$$v_w(x)=\sqrt{\frac{m+1}{-2}U_0\nu x^{m-1}}f(0)\propto x^{(m-1)/2}.$$

The similarity equation is obtained as follows:

$$f'''-ff''+\beta f'^2=0 \tag{9}$$

with the same BCs as Eq. (6a)–(6c). For this case, one obtains $2<\beta<\infty$. Since there is no general analytic solutions for the above similarity equations, Eqs. (5), (7), and (9) combined with the BCs (6a)–(6c) were solved by using the so-called shooting method [24] to convert the boundary value problem to an initial value problem. A fourth-order Runge–Kutta integration scheme was adopted to solve the applicable initial value problem.

3. Results and discussion

3.1. Theoretical analysis of the solutions

When $m=1$, the equation reduced to the results discussed by Miklavcic and Wang [20]. Therefore, it is found that the current formulation includes the solution for the shrinking sheet with a linear velocity. The solution is an exact solution for the whole Navier–Stokes equations only at $m=1$. For other power indices, the

boundary layer assumptions have to be employed. The discussion here will be emphasized on other parameters except $m = 1$. For Eq. (5) there is a special solution in the form of $f(\eta) = a_1/(\eta + a_2)$. Substituting this relationship into Eq. (5) yields

$$f(\eta) = \frac{\frac{6}{2-\beta}}{\eta + \sqrt{\frac{6}{2-\beta}}} \tag{10}$$

at $s = \sqrt{6/(2-\beta)}$. This solution is an algebraically decaying function with $f(\infty) \to 0$. For this case, $f''(0) = 2/(\sqrt{6/(2-\beta)})$. For a stretching sheet problem, there also exist algebraically decaying solutions as found by Liao and Magyari [25]. From Ref. [20], for $m = 1$, the analytical solution is

$$f(\eta) = C + \frac{e^{-Cx}}{C}, \tag{11}$$

where $C = f(\infty)$ and C can be obtained from the mass transfer parameter as $s = C + (1/C)$. Analytical solutions also exist for other power indices as follows. When $m = -1/3, \beta = -1$, Eq. (5) becomes

$$f''' + ff'' + f'^2 = 0. \tag{12}$$

This equation can be integrated twice as

$$f' + \frac{f^2}{2} = (\alpha - s)\eta + \left(\frac{s^2}{2} - 1\right), \tag{13}$$

where $\alpha = f'(0)$. Since from the BCs, for sufficiently large η, $f'(\infty) \to 0$. Then, it requires that $\alpha \geqslant s$. However, if $\alpha > s$, we obtain $f(\eta) \propto \sqrt{\eta}$ for $\eta \to \infty$, and is not finite. Therefore, in order to have a solution, it requires that $\alpha = s$. Then, we have

$$f' + \frac{f^2}{2} = \left(\frac{s^2}{2} - 1\right). \tag{14}$$

When $\eta \to \infty$, we have $f(\infty) = \sqrt{s^2 - 2}$. Therefore, for $\beta = -1, s \geqslant \sqrt{2}$. The lower limit is just the algebraically decaying solution for $s = \sqrt{2}$. The solution is

$$f(\eta) = \sqrt{s^2 - 2}\coth\left[\frac{\sqrt{s^2-2}}{2}\eta + \coth^{-1}\left(\frac{s}{\sqrt{s^2-2}}\right)\right] \tag{15a}$$

and

$$f'(\eta) = -\frac{s^2 - 2}{2}\operatorname{csch}^2\left[\frac{\sqrt{s^2-2}}{2}\eta + \coth^{-1}\left(\frac{s}{\sqrt{s^2-2}}\right)\right]. \tag{15b}$$

Another analytical solution can be obtained for $\beta = -2$, namely $m = -1/2$, then Eq. (5) becomes

$$f''' + ff'' + 2f'^2 = 0. \tag{16}$$

The above equation is equivalent to

$$\frac{1}{f}\frac{d}{d\eta}\left[f^{3/2}\frac{d}{d\eta}\left(f^{-1/2}f' + \frac{2}{3}f^{3/2}\right)\right] = 0. \tag{17}$$

Integrating once yields

$$-\frac{1}{2}f'^2 + ff'' + f^2f' = -\frac{1}{2} + s\alpha - s^2. \tag{18}$$

By applying the BCs at $\eta \to \infty$, we obtain $-\frac{1}{2} + s\alpha - s^2 = 0$. Then we know that solution exists for

$$\alpha = s + \frac{1}{2s}. \tag{19}$$

An integration of Eq. (18) yields

$$f^{-1/2}f' + \frac{2}{3}f^{3/2} = \frac{2}{3}s^{3/2} - \frac{1}{\sqrt{s}}. \tag{20a}$$

Using the BCs at $\eta \to \infty$, we know that $s \geqslant \sqrt{3/2}$, where the lower limit is also the algebraically decaying solution. By define a new function as $g(\eta) = \sqrt{f(\eta)}$ and substituting it into Eq. (20a) yields

$$g' + \frac{1}{3}g^3 = \frac{1}{3}s^{3/2} - \frac{1}{2\sqrt{s}}. \tag{20b}$$

The final solution reads

$$\eta + C_0 = \frac{1}{2a^2}\ln\frac{f - a\sqrt{f} + a^2}{(\sqrt{f} + a)^2} - \frac{\sqrt{3}}{a^2}\tan^{-1}\frac{2\sqrt{f} - a}{a\sqrt{3}}. \tag{21}$$

where $a = -\left(s^{\frac{3}{2}} - \frac{3}{2\sqrt{s}}\right)^{1/3}$ and

$$C_0 = \frac{1}{2a^2}\ln\frac{s - a\sqrt{s} + a^2}{(\sqrt{s} + a)^2} - \frac{\sqrt{3}}{a^2}\tan^{-1}\frac{2\sqrt{s} - a}{a\sqrt{3}};$$

It is an implicit function of η.

For large mass transfer parameters, define a new function as $f(\eta) = s + (\varphi(\omega)/s)$, where $\omega = \eta s$. Substituting this function into Eq. (5) and letting $s \to \infty$ yield

$$\dddot{\varphi} + \dot{\varphi} = 0 \tag{22}$$

with boundary conditions

$$\varphi(0) = 0, \tag{23a}$$

$$\dot{\varphi}(0) = -1, \tag{23b}$$

$$\dot{\varphi}(\infty) = 0. \tag{23c}$$

The solution is similar to the asymptotic suction profiles as

$$\varphi(\eta) = e^{-\eta s} - 1. \tag{24}$$

When $m = -1(+)$, $\beta \to -\infty$, the similarity equation is very interesting

$$f''' + f'^2 = 0 \tag{25}$$

the value of s does not affect the solution, because it is only a function of $f'(\eta)$. There is also a special analytical solution for Eq. (25) as

$$f(\eta) = \frac{6}{\eta + \sqrt{6}} + s - \sqrt{6}. \tag{26}$$

This solution is the only solution for Eq. (25). For this case $f''(0) = \sqrt{2/3}$. For $m = -1(-)$, $\beta \to +\infty$, it is obtained that $F''' + F'^2 = 0$ by using a transformation $f(\eta) = (1/\sqrt{\beta})F(\sqrt{\beta}\eta)$ for Eq. (9). The solution will be the same as that for $m = -1(+)$, which makes sense from the physical configuration.

3.2. Numerical solutions

3.2.1. Solutions for $\infty < \beta \leqslant 2$

Since there is no general analytical solution for the similarity equations, numerical technique has to be used to solve the boundary value problems. The code was validated using the previous reported values from Ref. [20] for $\beta = 1$. During the computation, the shooting error was controlled less than 10^{-6}.

The solution domains of Eq. (5) are shown in Fig. 1a and b under different values of β for $f''(0)$ and $f(\infty)$, respectively, as a function of mass suction parameter at the wall, namely it s. From Fig. 1 very rich non-linear phenomena can be observed for Eq. (5) with the associated BCs (6a)–(6c). Since the solution for some special parameters, for example, $\beta = -1$ and $\beta = -2$ have been discussed in previous section analytically, the results were not shown in the plot. For $\beta = 0$, Eq. (5) becomes the famous Blasius equation, the solution has been discussed in another work about Blasius equation [26]. Therefore, no solutions for $\beta = 0$ is shown in the result, but the solution behaviors are very similar to those for $\beta = 0.5$. From Fig. 1, it is found that solutions are not unique for certain values of β. For $\beta \geqslant 1$, there is one solution for a critical value of

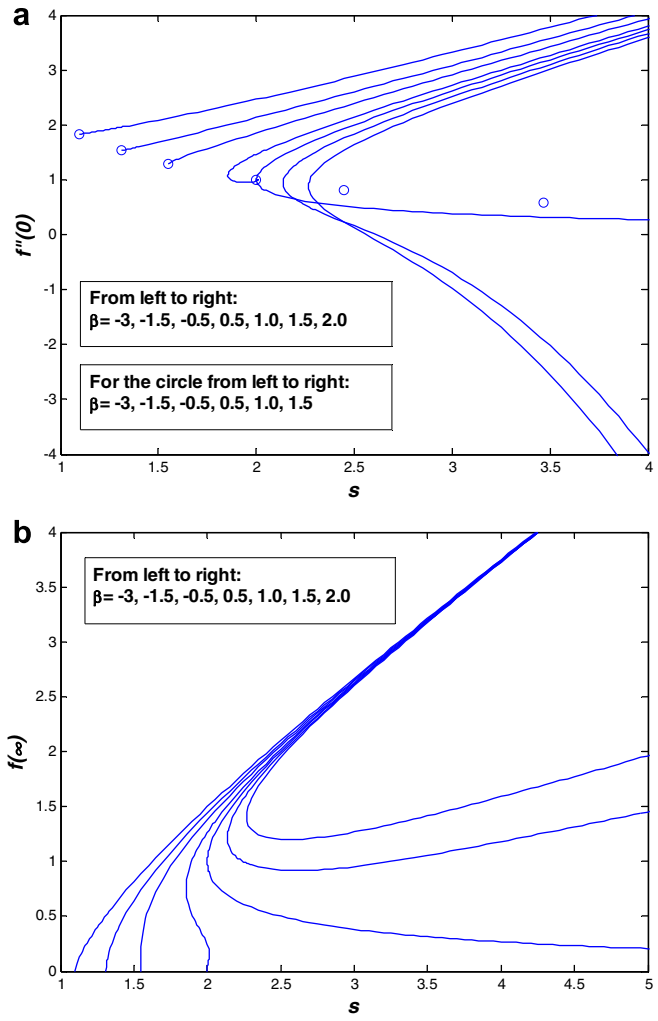

Fig. 1. The solution domain for the momentum boundary layer equation at different values of for $f''(0)$ and $f(\infty)$ in (a) and (b), respectively.

$s = s_c$, and two solutions for mass suction parameters higher than s_c. As a matter of fact, the algebraically decaying solution can be treated as the third solution, which is not in the solution domain curve as shown in Fig. 1a. Also when $\beta > 1$, for the lower solution branch, $f''(0)$ becomes negative when s is sufficiently large, which, in another words, means that there is velocity overshoot in the boundary layer. The fluid velocity near the sheet can be greater than the wall shrinking velocity. At the same time, there is a certain mass suction parameter making the wall shear stress zero. This is of practical interest in wall drag reduction for a shrinking sheet. However, quite different solution behavior is seen for $0 < \beta < 1$. The result of $\beta = 0.5$ gives a typical example. For this domain of β, there also exist multiple solutions. However, the lower solution branch terminates at a finite value of s. The terminating point is just the solution of Eq. (10), namely the algebraically decaying solution, which is also shown in Fig. 1a with a circle. The behavior near the terminating point is very complicated. There is a spiral with infinitely many solutions when it approaches the termination point. This kind of solution behavior has been discussed by Miklavcic and Wang [20] for the axisymmtric case in their paper. Similar behaviors were observed in the current study for $0 < \beta < 1$. For $\beta = 0$, the behavior is also similar as discussed in another work [26]. But for $\beta < 0$, the solution domain becomes simpler. There is only one solution branch and the solution branch terminates at the algebraically decaying solution points as indicated by the circles. For the upper solution branch, $f''(0)$, namely the wall shear stress, increases with the decrease of β and generally increase with the increase of mass suction at the wall.

The variation behavior of $f(\infty)$ is also quite interesting for different values of β as shown in Fig. 1b. $f(\infty)$ can give a measure of the total flow rate induced by the shrinking sheet and is important in practical applications. For $\beta \geqslant 1$, the values of $f(\infty)$ for both solution branches are greater than zero. Only the algebraically decaying solution leads to a zero value of $f(\infty)$. For lower solution branch, as proved by Miklavcic and Wang [20], when $\beta = 1$, $f(\infty)$ continuously decrease when s increases. However, for $\beta > 1$, there is a minimum value of $f(\infty)$ for the lower solution branch under a certain mass suction parameter. This mass suction parameter corresponds to the shear-free mass suction parameter for the lower solution branch. When s is larger than this critical value, the induced flow rate increases with increasing s. This increase in induced flow rate is believed due to the fluid velocity overshoot in the boundary layer. When $\beta < 1$, the solution curve terminates at the algebraically decaying solution with $f(\infty) = 0$. For the upper solution branch, $f(\infty)$ is always increasing with the increase of mass suction parameter, s.

In order to show the velocity and shear stress in the boundary layer, some typical examples are shown in Fig. 2 for different values of β with $s = 2.5$ for the upper branch. It is seen that for the upper solution branch under the same mass suction at the wall, the boundary layer is closer to the wall for a lower value of β. The wall drag also increases with the decrease of β. Some solutions of the lower solution branch for $\beta = 1.5$ under different suction parameters are shown in Fig. 3. Interesting variation behavior is found in Fig. 3 for the lower solution branch. As the mass suction parameter increases, the shear stress becomes more negative with velocity overshoot near the shrinking sheet. The shear stress profiles in the boundary layer are no longer monotonously decreasing as the upper solution branch. The maximum magnitude of shear stress can occur in the boundary layer or on the wall. But for the upper solution branch, the maximum shear stress always occurs on the wall. Due to wall mass suction, the fluid can actually drag the sheet to shrink into the slot. The physical implementation of the lower solution branch is of interest for further investigation.

3.2.2. Solutions for $2 < \beta < \infty$

For this range of β, the shrinking sheet is moving toward the slot with a rapidly decreasing velocity with the distance from the slot.

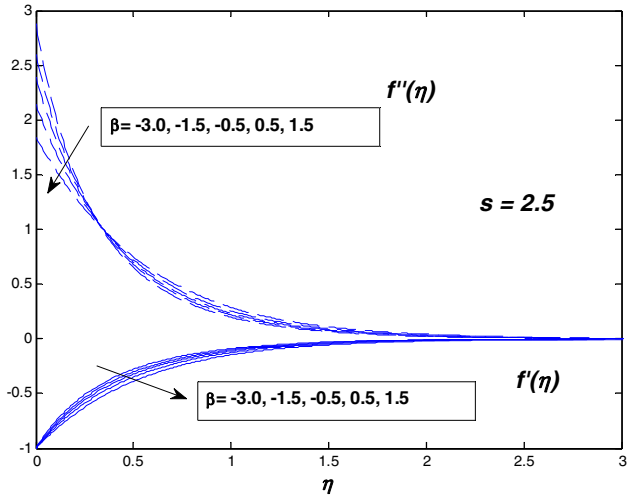

Fig. 2. Some examples of the velocity and shear stress profiles in the boundary layers under different values of β.

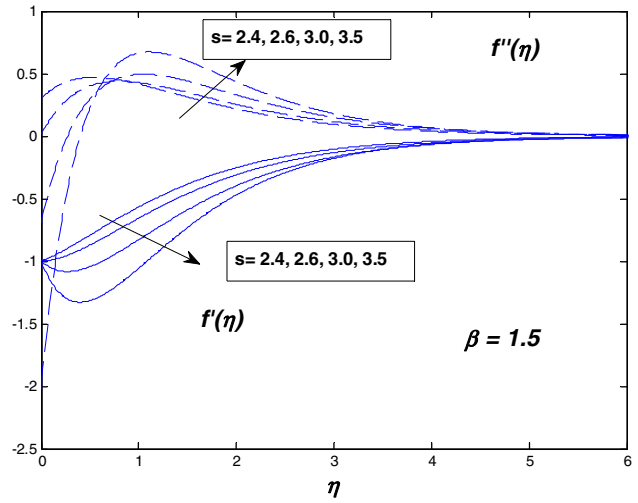

Fig. 3. Some examples of the velocity and shear stress profiles with over shoot in the boundary layers under different values of mass suction at $\beta = 1.5$.

Even though Eq. (5) with BCs (6a)–(6c) has solutions also for $2 < \beta < \infty$, the solution does not connect to any meaningful value of power index m for a shrinking sheet. For this case, based on the definition of the velocity, a positive s indicates mass injection and a negative value implies mass suction. There is also a general algebraically decaying solution for Eq. (9) as

$$f(\eta) = \frac{\frac{6}{\beta-2}}{\eta + \sqrt{\frac{6}{\beta-2}}} \tag{27}$$

at $s = \sqrt{6/(\beta-2)}$. It interestingly shows that solutions exist for a mass injection at the wall with an algebraically decaying function, which is quite different from a non-rapid shrinking sheet. The numerical solutions of Eq. (9) together with BCs (6a)–(6c) were computed for certain values of β. The solution domain for $\beta = 6$ and $\beta = 10$ are shown in Fig. 4. Interesting observations are found. For each value of β, there are two solution branches. Both branches terminate at the same point, which is just the algebraically decaying solution for that value of β. Solutions exist for positive values of s, indicating that there is solution for mass injection at the wall for this rapid shrinking sheet. Based on Eq. (27), it is expected that the solution branch terminating points moves toward the left with increasing values β of and reach $s = 0$ for $\beta \to \infty$. The values of $f''(0)$ changes with the change of β. For the lower solution branch, a higher value of β leads to a higher value of $f''(0)$, showing higher wall shear stresses. However, for the upper solution branch, there are some interception point for different values of β. When s is less than a certain value, a higher β results in a smaller wall stress. However, when s is large than that value, a higher β leads to a higher wall stress. As both solution branches approach to the terminate points the difference between the two solutions becomes smaller and smaller. The solution multiplicity and similar solution behavior have been found for a stretching sheet by Liao [19]. The values of $f(\infty)$ are also illustrated in Fig. 4. From the solution, it is found that the lower solution branch gives a more negative number of $f(\infty)$, meaning a higher magnitude with more induced flow rate. For the lower branch, a higher value of β results in a lower induced flow rate, namely a higher value of $f(\infty)$ with less magnitude. But for the upper solution branch, there also exists an interception point and the variation trend changes when that point is passed. As the solutions branches approach the terminating point, $f(\infty)$ goes to zero for both solution branches.

To further show the velocity and the shear stress variation behavior across the boundary layers, some velocity and shear stress profiles are presented briefly. Some examples for the solution with $\beta = 6$ at different values of s are shown in Figs. 5 and 6 for the lower solution branch and the upper solution branch, respectively. For the lower solution branch, all the three functions like $f(\eta)$, $f'(\eta)$, and $f''(\eta)$ are monotonous functions either increasing or decreasing with η. The maximum wall shear stress and velocity occur on the wall. With the increase of s, the solution decays slower with further penetration to the fluid far from the shrinking sheet. Boundary layer thickness becomes thicker. There is no velocity overshoot found for this solution branch. However, very different observations are seen in the upper solution branch as shown in Fig. 6. The main difference of the upper solution branch from the lower branch is the velocity or shear stress over shoot in the boundary layer. But the overshoot in this condition is different from what we found in the previous sections. This velocity overshoot occurs in the boundary layer with positive fluid velocity. In another word, compared to the sheet shrinking velocity, there is a reversal flow in the boundary layer near the edge of the boundary layer. This reversal flow makes the flow induced by the shrinking sheet penetrate deeper into the fluid with thicker boundary layer thickness compared with the lower solution branch. With the

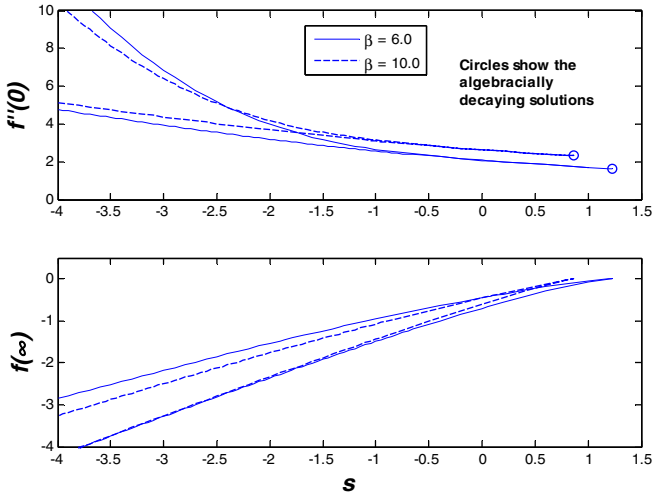

Fig. 4. The solution domain for the momentum boundary layer equation at different values of β for $f''(0)$ and $f(\infty)$ for the conditions with a rapid decreasing velocity.

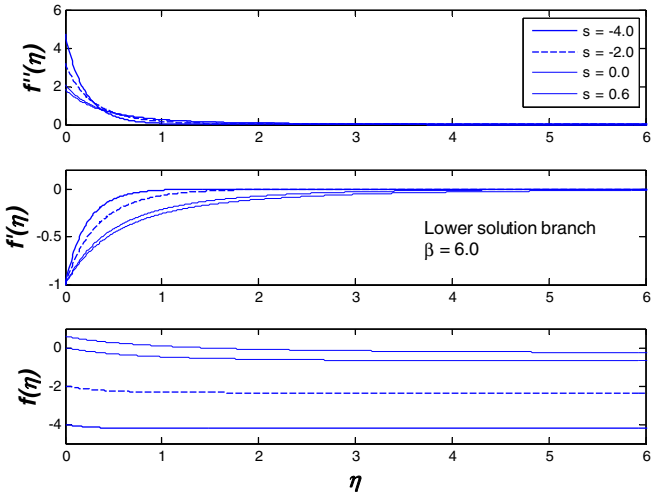

Fig. 5. Some examples of the solution for the lower solution branch at $\beta = 6.0$ with rapid decreasing velocity under different mass transfer parameters.

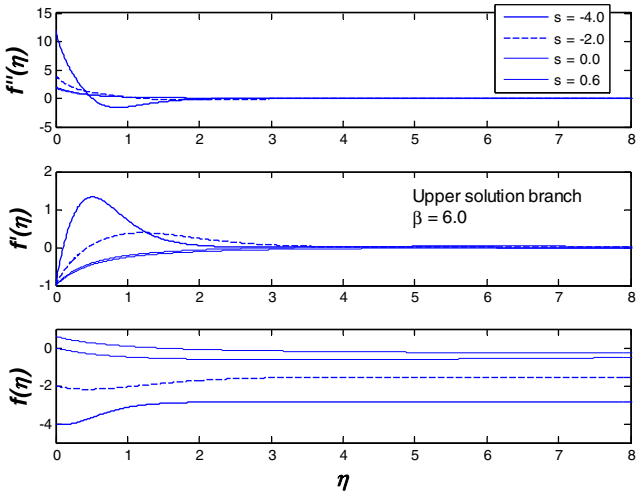

Fig. 6. Some examples of the solution for the upper solution branch at $\beta = 6.0$ with rapid decreasing velocity under different mass transfer parameters, where velocity or shear stress over shoot near the edge of the boundary layer is clearly observed.

increase of s, the boundary layer thickness also increases like the lower solution branch.

In a short summary, the shrinking sheet with a power-law velocity at the sheet is investigated in this work. Since as pointed out by previous researchers [14,16], the exponentially stretching velocity also belongs to such group of similarity equations, the current results can also applied to an shrinking sheet with exponentially shrinking velocity by taking $\beta = 2$. It should be noted that for rapid shrinking sheet, the solution variation behaviors are quite different from the rapidly stretching surface, where there are infinite number of solutions for certain mass transfer parameter with mass suction [16]. But for the rapidly shrinking sheet problem, solutions can exists with mass injection and there are only two solutions found by numerical techniques. Compared with the continuously stretching surface, the boundary layer flow for a continuously shrinking sheet is quite different and interesting non-linear phenomena were found. However, from the physical implementation point of view, whether these flows exist in a real world is still an open problem worthy of further study.

4. Conclusion

In this paper, the momentum boundary layers over a continuously shrinking surface with a power-law velocity were investigated. Some findings can be summarized as follows:

1. An algebraically decaying solution is found analytically for each value of the controlling parameter β under a certain value of the mass transfer parameter s.
2. Two solution branches exist for $\beta \geqslant 1$. There is also an algebraically decaying solution for this range of β. Quite different boundary layers were found for the two solution branches for $\beta > 1$ with velocity overshoot seen for the lower solution branch for sufficiently large mass suction parameter.
3. For $0 \leqslant \beta < 1$, there are also more than one solutions for certain mass suction parameters. But the lower solution branch always terminates at the algebraically decaying solution. The solution behavior is quite interesting and very complicated when the solution domain approaches to the terminating point.
4. For $\beta < 0$, there exist one solution and the solution domain terminates at the algebraically decaying solution. Exact solutions are presented for some special cases with $m = -1$, $\beta = -1$, and $\beta = -2$.
5. For $2 < \beta < \infty$, the boundary layers are corresponding to the rapidly decreasing case. There are two solutions obtained for certain mass transfer parameters. Both solution branches terminate at the same point, namely the algebraically decaying solution. Velocity overshoot near the boundary layer edge is found for the upper solution branch. It is also distinct from the stretching sheet with a rapidly decreasing velocity that solution exists for mass injection;
6. The boundary layers over a shrinking sheet are greatly different from the boundary layers due to a stretching sheet and offer more nonlinear phenomena in the boundary layer theory.

Acknowledgement

The author expresses his sincere appreciation to the reviewers for their time and interest in the work and valuable suggestions and comments.

References

[1] T. Altan, S. Oh, H. Gegel, Metal Forming Fundamentals and Applications, American Society of Metals, Metals Park, OH, 1979.
[2] E.G. Fisher, Extrusion of Plastics, Wiley, New York, 1976.
[3] Z. Tadmor, I. Klein, Engineering Principles of Plasticating Extrusion, Polymer Science and Engineering Series, Van Norstrand Reinhold, New York, 1970.
[4] B.C. Sakiadis, Boundary-layer behavior on continuous solid surface: I. Boundary-layer equations for two-dimensional and axisymmetric flow, J. AIChe. 7 (1961) 26–28.
[5] B.C. Sakiadis, Boundary-layer behavior on continuous solid surface: II. Boundary-layer equations for two-dimensional and axisymmetric flow, J. AIChe 7 (1961) 221–225.
[6] F.K. Tsou, E.M. Sparrow, R.J. Goldstain, Flow and heat transfer in the boundary layer on a continuous moving surface, Int. J. Heat Mass Transfer 10 (1967) 219–235.
[7] L.J. Crane, Flow past a stretching plate, Z. Angew. Math. Phys. 21 (4) (1970) 645.
[8] W.H.H. Banks, Similarity solutions of the boundary-layer equations for a stretching wall, J. Mech. Theor. Appl. 2 (1983) 375–392.
[9] B.K. Dutta, P. Roy, A.S. Gupta, Temperature field in flow over a stretching sheet with uniform heat flux, Int. Comm. Heat Mass Transfer 12 (1985) 89–94.
[10] L.J. Grubka, K.M. Bobba, Heat transfer characteristics of a continuous stretching surface with variable temperature, ASME J. Heat Transfer 107 (1985) 248–250.
[11] C.K. Chen, M.I. Char, Heat transfer of a continuous stretching surface with suction and blowing, J. Math. Anal. Appl. 135 (1988) 568–580.
[12] M.E. Ali, On thermal boundary layer on a power law stretched surface with suction or injection, Int. J. Heat Fluid Flow 16 (1995) 280–290.
[13] E.M.A. Elbashbeshy, Heat transfer over a stretching surface with variable surface heat flux, J. Phys. D 31 (1998) 1951–1954.
[14] E. Magyari, B. Keller, Heat and mass transfer in the boundary layers on an exponentially stretching continuous surface, J. Phys. D 32 (5) (1999) 577–585.
[15] E. Magyari, B. Keller, Exact solutions for self-similar boundary-layer flows induced by permeable stretching walls, Eur. J. Mech. B 19 (1) (2000) 109–122.
[16] E. Magyari, M.E. Ali, B. Keller, Heat and mass transfer characteristics of the self-similar boundary-layer flows induced by continuous surfaces stretched with rapidly decreasing velocities, Heat Mass Transfer 38 (1–2) (2001) 65–74.
[17] S.K.S. Boetcher, E.M. Sparrow, J.P. Abraham, Numerical simulation of the radiative heating of a moving sheet, Numer. Heat Transfer A 47 (1) (2005) 1–25.
[18] S.J. Liao, A new branch of solutions of boundary-layer flows over a stretching flat plate, Int. J. Heat Mass Transfer 49 (12) (2005) 2529–2539.
[19] S.J. Liao, A new branch of solution of boundary-layer flows over a permeable stretching plate, Int. J. Non-Linear Mech. 42 (2007) 819–830.
[20] M. Miklavcic, C.Y. Wang, Viscous flow due to a shrinking sheet, Quart. Appl. Math. 64 (2) (2006) 283–290.
[21] T. Hayat, Z. Abbas, M. Sajid, On the analytic solution of magnetohydrodynamic flow of a second grade fluid over a shrinking sheet, J. Appl. Mech. Trans. ASME 74 (6) (2007) 1165–1171.
[22] M. Sajid, T. Hayat, T. Javed, MHD rotating flow of a viscous fluid over a shrinking surface, Nonlinear Dyn. 51 (1–2) (2008) 259–265.
[23] S. Goldstein, On backward boundary layers and flow in converging passages, J. Fluid Mech. 21 (1965) 33–45.
[24] F.M. White, Viscous Fluid Flow, second ed., McGraw-Hill, New York, 1991.
[25] S. Liao, E. Magyari, Exponentially decaying boundary layers as limiting cases of families of algebraically decaying ones, Z. Angew. Math. Phys. 57 (2006) 777–792.
[26] T. Fang, W. Liang, C.F. Lee, A new solution branch for the Blasius equation, Comput. Math. Appl. (submitted for publication).